

An Upgraded Red Channel for the Palomar Double Spectrograph

Evan N. Kirby^{1,2}
and
Gustavo Rahmer^{1,3}

ABSTRACT

The Palomar Double Spectrograph (DBSP) was installed on the Hale 200-inch telescope in 1982, and its red channel was last refurbished in 1995. In order to modernize the instrument and provide new capabilities, we replaced the red channel's detector with a deep-depletion CCD manufactured by Lawrence Berkeley National Laboratories. This change increased the spectrograph's throughput by a factor of 1.5 between 5500 Å and 8000 Å, and well over a factor of 2 at redder wavelengths. The throughput peaks at 37%, remains above 20% through 9500 Å, and remains above 5% through 10200 Å. Because the chip is longer, the spectral range in a single exposure was increased by a factor of 2.5. The new red channel entered into service on 2011 October 27.

Subject headings: instrumentation: detectors — instrumentation: spectrographs

1. Introduction

Oke & Gunn (1982) built and commissioned the Palomar Double Spectrograph (DBSP), a low- to moderate-resolution spectrograph at the Cassegrain focus of the Hale 200-inch telescope. The spectrograph has red and blue channels, separated by a dichroic filter. It is capable of simultaneous spectroscopy of the entire optical spectrum, from the atmospheric cut-off at 3200 Å to beyond 1 μm. Spectral range and resolution for each channel may be adjusted by changing the dispersions for each of the two channels from the suite of available gratings.

The basic design for DBSP has not changed

¹California Institute of Technology, 1200 E. California Blvd., MC 249-17, Pasadena, CA 91125

²Hubble Fellow.

³Large Binocular Telescope Observatory, 933 North Cherry Avenue, Tucson, Arizona 85721

over the past three decades. However, the blue and red channels have been upgraded separately several times each. The original RCA 320 × 512 CCD on the blue channel was replaced four times. The subsequent detectors were a thinned Texas Instruments 800 × 800 CCD (1987); a thinned, anti-reflection-coated Tektronix 1024 × 1024 CCD (1994); a thinned, ultraviolet-flooded Loral 2688 × 512 CCD (2002); and a thinned, anti-reflection-coated E2V 4096 × 2048 CCD (2005), which is presently in operation. The red channel's first overhaul occurred in 1995. The original camera between the collimator and the detector was replaced with a seven-element design by Harland Epps of the University of California/Lick Observatories. The original Texas Instruments 800 × 800 CCD was replaced with a thinned, anti-reflection-coated Tektronix 1024 × 1024 CCD. That detector was in use until this upgrade.

In early 2010, the director of Caltech Optical Observatories, which operates the Hale telescope, made modernization of DBSP's red channel a top priority. On 2011 October 27, we completed that upgrade. ENK served as the project scientist, and GR served as the project manager and detector specialist. In this paper, we describe the science cases that will benefit from this upgrade (Section 2), the requirements for the upgrade (Section 3), the changes made to the instrument (Section 4), and the measured changes in its performance (Section 5).

2. Science Cases

When the Short Wavelength Integral Field Spectrograph (SWIFT) was commissioned at Palomar (Thatte et al. 2010), that project provided a spare CCD to Caltech Optical Observatories. The deep-depletion detector has high throughput to wavelengths beyond $1 \mu\text{m}$. This detector was made available for the DBSP upgrade.

To make the most of this available, in-house CCD, DBSP users of the previous five years were surveyed in February 2010 about their wishes for an upgraded instrument. The survey solicited general feedback as well as specific benefit to science goals from a red detector with increased throughput and spectral range. The responses to the survey showed that 75% of DBSP users would benefit from increased throughput for the red channel. Nearly all of those users stated that they would also benefit from the increased spectral range. The results of this survey informed the requirements of the upgrade (Section 3).

The following list is an assortment of science cases helped by the new red detector. This list is highly abbreviated. Naturally, any observations in the wavelength range $4800 \text{ \AA} \lesssim \lambda \lesssim 10500 \text{ \AA}$ will be improved by the increased quantum efficiency of the new

CCD.

2.1. Solar System Objects

The Hale telescope routinely hosts planetary physicists, many of whom use DBSP. For example, Buratti et al. (2002) concluded from DBSP spectra that the low albedo of some Saturnian moons results from settling of exogenous dust with an asteroid-like composition. In another study, Weissman et al. (2008) found that the composition of the asteroid 2867 Steins (possibly including the mineral oldhamite) does not match any meteorite. They also found a difference in spectral energy distribution between different hemispheres of the asteroid. This study relied on time-resolved spectroscopy. Therefore, it was important to collect many photons in a short period of time. These and other planetary studies will enjoy the greater efficiency afforded by DBSP's new red channel.

2.2. Cataclysmic Variables

Unambiguously identifying synchrotron emission requires the observation of multiple harmonics. Wide coverage of the optical spectrum is helpful for this purpose. For example, Bhalerao et al. (2010) observed a cataclysmic variable with Keck/LRIS (Oke et al. 1995) and DBSP in order to measure the synchrotron frequency, from which the magnetic field strength was deduced. They also measured a radial velocity curve, from which they derived the mass ratio of the M dwarf to the white dwarf. DBSP's new red detector will aid measurements of both the magnetic field strength and mass ratio. The identification of synchrotron emission depends on identifying at least several peaks, which can occur deep into the red part of the optical spectrum. Furthermore, the CCD's increased sensitivity permits higher signal-to-noise ratios of the few narrow features from which radial velocities can be measured in M dwarfs, such as the

Na I doublet at 8190 Å.

2.3. Late-Type Dwarf Stars

The photometric Y -band centered at $1.035 \mu\text{m}$ hosts many of molecular absorption bands whose strength is very sensitive to stellar spectral type (Hillenbrand et al. 2002). Stars of later spectral type have stronger absorption in these bands. Some of the strongest molecular features in the Y -band are TiO, VO, and FeH (see Section 2.4). Other very red features in substellar objects such as T dwarfs include CrH, H₂O, and Cs I lines (Kirkpatrick et al. 1999; Burgasser et al. 2003). Therefore, DBSP’s increased sensitivity in the far red will aid in spectrally typing low-mass stars and substellar objects.

2.4. Initial Mass Function in Elliptical Galaxies

Wing & Ford (1969) discovered a molecular absorption band near 9910 Å in cool dwarfs, but they could not identify the responsible molecule. Even before Nordh et al. (1977) suggested that iron hydride (FeH) was the molecule, Whitford (1977) found that the band was highly sensitive to stellar atmospheric pressure or surface gravity. Later that year, Wing et al. (1977) confirmed that FeH is the absorbing species. The pressure sensitivity of the band means that its strength in the spectrum of the integrated light from a galaxy could indicate the ratio of low-mass, high-pressure stars to high-mass, low-pressure stars. In other words, the Wing-Ford band is a probe of the stellar initial mass function (IMF). Recently, van Dokkum & Conroy (2010) used this band in conjunction with the Na I doublet at 8190 Å to argue that large elliptical galaxies exhibit a steeper-than-expected IMF. DBSP’s increased sensitivity in the region of the Wing-Ford band now makes the Hale telescope the ideal venue to confirm van Dokkum & Conroy’s measure-

ment and extend it to a broader sample of galaxies.

2.5. Galactic Emission Lines

A boost in sensitivity enables spectroscopic detection of galaxies of lower luminosity at a given redshift. Additionally, the extended spectral range of the upgraded red channel of DBSP increases the redshift range accessible from strong, well-studied emission lines, such as [O II] $\lambda 3727$ (e.g., Wu et al. 2011). For example, the [O II] doublet was difficult to observe with the old detector at $z > 1.28$. With the new detector, [O II] is observable to slightly beyond $z = 1.82$.

3. Requirements

The science cases informed the following requirements for the upgrade of the red channel of DBSP.

1. Throughput: Provide a spectrograph throughput of $> 25\%$ from 5500 Å to 9400 Å and $> 10\%$ from 9400 Å to $1 \mu\text{m}$.
2. Accessible spectrum: Extend the red wavelength limit of useful data from $\sim 850 \text{ nm}$ to $1 \mu\text{m}$.
3. Spectral range: Maintain or increase the spectral range. The previous detector was 25 mm long, corresponding to 1340 Å of spectral coverage with a 600 line mm^{-1} grating.
4. Read time: Read out the illuminated portion of the detector in less than 30 s.
5. Read noise: Provide a read noise of less than $3 e^-$ per pixel.
6. Fringing: Eliminate almost all red fringing.

At the time of commissioning, we achieved all of these goals except item 5 (see Section 5).

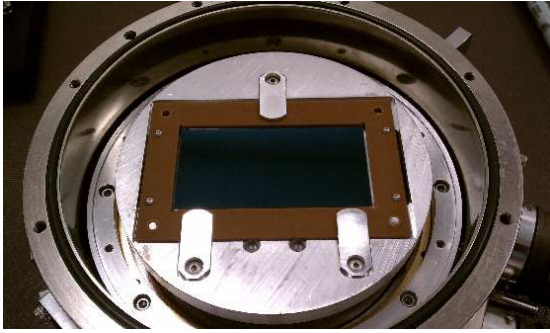


Fig. 1.— The new detector for the red channel mounted on the end of the new dewar. The detector mask and the dewar end cap have been removed.

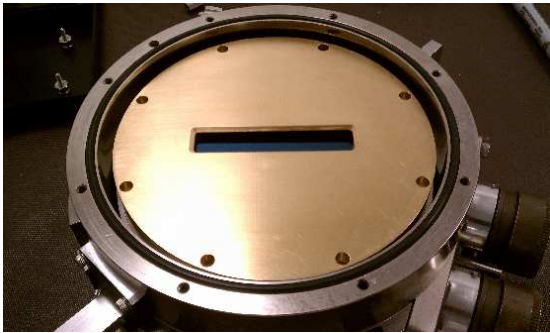


Fig. 2.— The new detector with the detector mask installed. The mask acts as a radiation shield, reflecting all light except the spectrally dispersed image of the slit.

4. New Detector and Dewar for the Red Channel

The spare CCD for the SWIFT integral field unit was adopted for this project. The detector was manufactured and packaged at Lawrence Berkeley National Laboratories (LBNL). The silicon is $250\ \mu\text{m}$ thick and fully depleted. The thickness offers excellent sensitivity in the far red and virtually eliminates fringing. This device is identical to the two CCDs used in SWIFT (Thatte et al. 2010). The detector, but not its packaging, is also similar to the two LBNL CCDs recently installed in Keck/LRIS (Rockosi et al. 2010).

Table 1 compares characteristics of the CCDs for the present blue channel, the previous red channel, and the new red channel.

This upgrade affected only the dewar for the red channel. We did not modify any part of the spectrograph’s optics except for the dewar window. We manufactured a new dewar rather than modifying the old one. This approach allowed for minimum interruption of scientific use of DBSP, which is a very popular instrument at the Hale telescope. We commissioned the upgrade in one night. At no time was DBSP unavailable for science. It also provided us the ability to return the old dewar and the old detector to service in the event of a problem with the new detector. This contingency has not been necessary.

The new dewar was designed and built by Infrared Laboratories of Tucson, Arizona, following our specifications. One of the primary goals of the new dewar was to increase the liquid nitrogen hold time while keeping the dewar’s size within the envelope allowed by the restrictive clearance of the Hale telescope’s Cassegrain cage. The size of the tank was increased and the location of the filling pipe was offset from its usual center position to minimize spilling when tilted during night operations. Two types of getters, substances that adsorb gases to maintain the vacuum, were used. Activated charcoal was permanently mounted on a container in direct contact with the liquid nitrogen tank. It adsorbs gases when cold. Zeolite was placed in a container attached to the exterior wall of the dewar. Because Zeolite eventually saturates and requires occasional re-generation, the container was designed to be accessible without opening the dewar. Another major improvement over the previous dewar was the design of the radiation shield to minimize openings, including the mask between the CCD and the entrance window and the use of gold plated surfaces around the detector mount. These enhance-

TABLE 1
DBSP DETECTOR CHARACTERISTICS

Characteristic	Current Blue Channel	Previous Red Channel	New Red Channel
Put in Service	2005	1995	2011
Manufacturer	E2V	Tektronix	LBNL
Dimensions (pixels)	4096 × 2048	1024 × 1024	4096 × 2048
Pixel Size (μm)	15	24	15
Read time (s) ^a	22	17	24 ^b
Read noise (e^-)	2.5	7.5	8
Plate scale (arcsec pixel ⁻¹)	0.389	0.468	0.293

^aRead times are specified for reading only the illuminated portion of the detectors.

^bThe read time is 12 s with the recommended 1×2 binning.

ments resulted in a hold time of more than 24 hours.

A new larger entrance window was designed following the prescription of the 1995 re-design of the red channel’s camera. That design assumed a flat focal plane. Because the previous detector was bowed, the new flat CCD improved the previous strong focus variation along the detector.

Like the blue camera, the red camera illuminates only a portion of the CCD. The spectrum covers the entire length of the CCD (4096 pixels) but only 440 of the 2048 pixels in the spatial axis. To save read time and hard disk space, only the illuminated portion of the detector (about 9×10^5 pixels) are read out.

5. Performance

The new red channel saw first light on 2011 October 27. Although the entire night was allocated to the commissioning of the red channel and new software for the slit viewing camera, we required just four hours for engineering. The six remaining dark hours were used for science observations.

The target for the first on-sky exposure was the spectrophotometric standard BD +28 4211. Figure 3 shows the 120 s exposure. The reddest wavelength visible in this spectrum is 10965 Å. Although the quantum efficiency of the detector is low at this wavelength, it is not zero. Flux from the $V = 10.5$ star is still strong at the very end of the chip. In the last column, the stellar profile peaks at 330 counts ($920 e^-$) above the background.

This exposure was one of several used to measure the red channel’s throughput. During 2010, we asked different observers to obtain spectra of spectrophotometric standard stars. On 2010 May 7, C. Scarlata observed Feige 34 using a grating ruled at 158 lines mm^{-1} and blazed at 7560 Å (158/7560 grating). She obtained one exposure at 10 s and another at 60 s through a 10” slit in photometric conditions. On 2010 May 12, T. Boroson observed BD +28 4211 using the 600/9500 grating. He obtained three 20 s exposures through a 10” slit in photometric conditions. We repeated these observations with the upgraded detector. We obtained two 120 s exposures of BD +28 4211 on 2011 Oc-

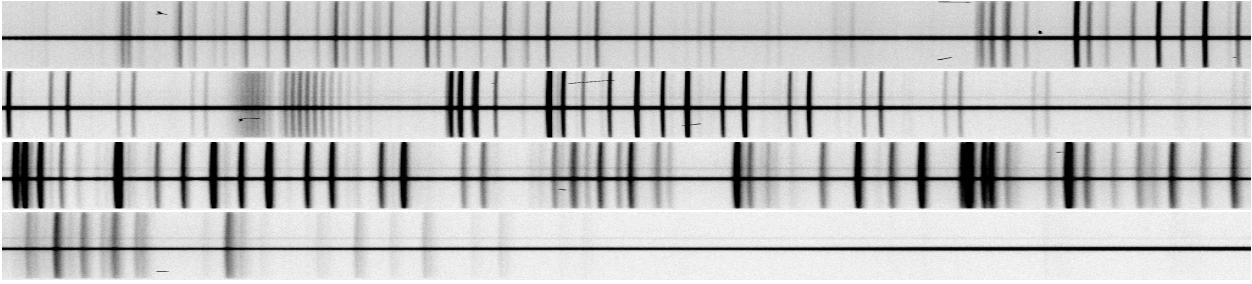


Fig. 3.— First light of the new red detector of DBSP. This is a 120 s exposure of the spectrophotometric standard BD +28 4211. Wavelength increases from left to right. The spectrum continues from the right end of each of the first three rows to the left end of the next row. The bluest and reddest wavelengths are 7635 Å and 10965 Å. The flux is scaled logarithmically. Each row is 2' high.

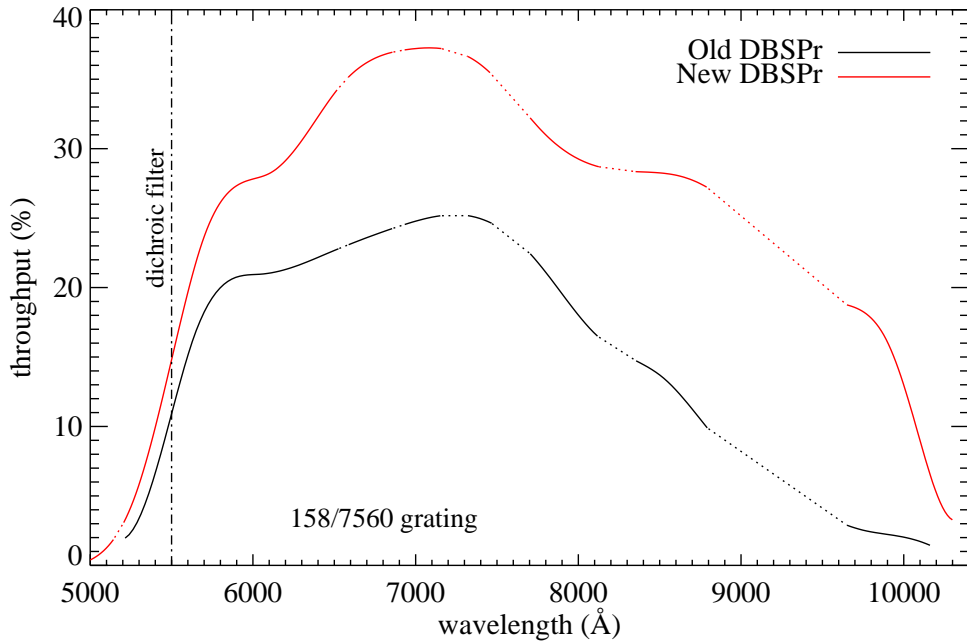


Fig. 4.— Spectroscopic throughput of the new red channel of DBSP with the 158 lines mm^{-1} grating with a blaze wavelength of 7560 Å. The losses from the atmosphere and the primary and secondary telescope mirrors have been removed. A dichroic filter with a cut-on wavelength of 5500 Å truncates the flux blueward of that wavelength. The red limit of the new CCD's throughput curve is imposed by the tabulation of the standard star (Massey & Gronwall 1990), not by the CCD. These curves were computed from observations of the spectrophotometric standard star Feige 34. The black curve is from an observation on 2010 May 7, before the upgrade. The red curve is from 2011 October 30, after the upgrade. Dotted portions of the curve indicate interpolation over regions of strong molecular absorption from the terrestrial atmosphere.

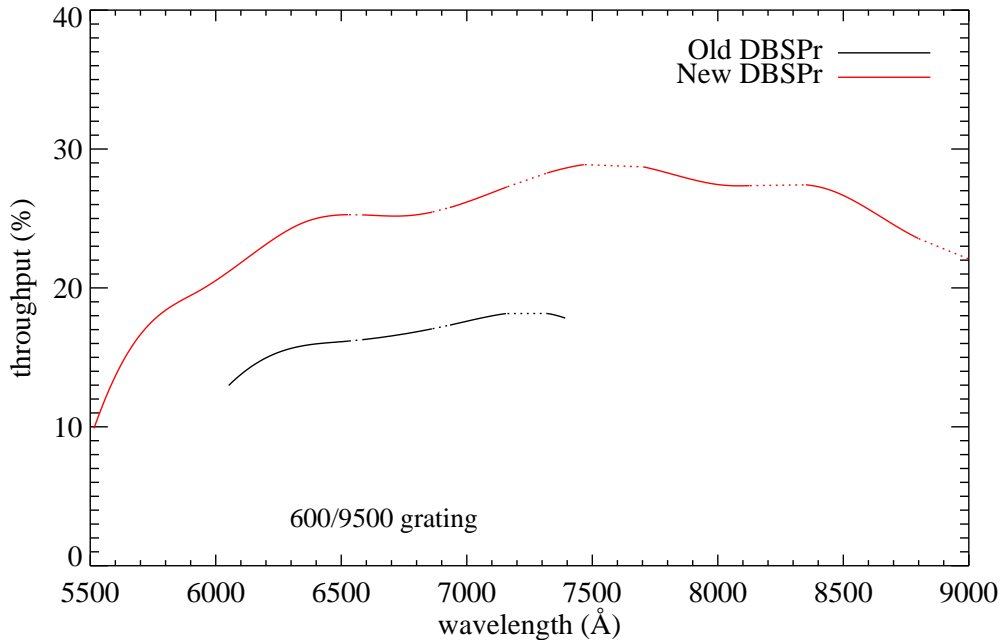


Fig. 5.— Spectroscopic throughput of the new red channel of DBSP with the 600 lines mm^{-1} grating with a blaze wavelength of 9500 Å. These curves were computed from observations of the spectrophotometric standard star BD +28 4211. The black curve is from an observation on 2010 May 12, before the upgrade. The red curve is from 2011 October 27, after the upgrade. The other details are the same as in Figure 4.

tober 27 in the same configuration used on 2010 May 12. S. Tendulkar observed Feige 34 on 2011 October 30 in the same configuration used on 2010 May 7 except that he used a 1.5" slit in 2" seeing. We corrected for slit losses, as described below.

We extracted one-dimensional spectra from the image frames using the NOAO `doslit` software package in IRAF¹. First, we removed the bias level with the CCD overscan region. We did not implement a flat field correction. We traced the spectrum and drew a broad extraction window around the trace that extended well into the background. Then, we

¹IRAF is distributed by the National Optical Astronomy Observatory, which is operated by the Association of Universities for Research in Astronomy (AURA) under cooperative agreement with the National Science Foundation.

extracted the spectrum and subtracted the sky background. Finally, we performed wavelength calibration from an exposure of He, Ne, and Ar arc lamps. The one-dimensional spectrum was a record of the number of photons counted by the spectrograph in each wavelength bin.

The number of photons per wavelength bin impinging on the primary mirror may be calculated with the following formula:

$$N_{\text{photons}} = \frac{t_{\text{exp}} A \Delta\lambda 10^{-0.4(m_{\text{AB}}+48.60)}}{h \lambda} \quad (1)$$

where t_{exp} is the total exposure time in seconds, $A = 1.76 \times 10^5 \text{ cm}^2$ is the area of the Hale telescope's primary mirror, $\Delta\lambda$ is the size of the wavelength bin, m_{AB} is the AB magnitude of the star, h is Planck's constant, and λ

is the wavelength. Oke (1990) tabulated m_{AB} for Feige 34 up to 9200 Å. Massey & Gronwall (1990) filled in the remaining spectrum from 9700 Å to 10200 Å. Massey et al. (1988) tabulated the flux for BD +28 4211 up to 8190 Å. Massey & Gronwall (1990) extended the spectrum to 10200 Å with a gap between 8900 Å and 9700 Å due to terrestrial atmospheric absorption.

The spectrograph throughput is simply the ratio of photons detected to the number of photons entering the slit. We corrected the throughput for atmospheric extinction with Hayes & Latham’s (1975) measurement of the extinction curve for Palomar Observatory. We also corrected for the reflections off the primary and secondary mirrors using the measured spectral reflectivity of aluminum (Weaver & Frederikse 2010). We also corrected the spectrum of Feige 34 from 2011 October 30 for slit losses. We computed the amount of light lost by comparing the measured throughput from the blue channel for the different dates. We divided the throughput curve for the red channel by this loss factor.

The Hale telescope’s primary mirror was re-aluminized in mid-October 2011. Therefore, some of the increase in throughput that we measured was due to the extra reflectivity of the primary mirror in addition to the larger quantum efficiency of the new CCD. Comparison of the blue channel’s throughput before and after mid-October suggests that the re-aluminizing increased the total efficiency by a few percent. Therefore, the re-aluminizing improved the throughput much less than the detector upgrade.

Figures 4 and 5 show the throughput curves for the two different configurations of the red channel. The curves are shown before and after the detector upgrade. The average improvement in throughput between 5500 Å and 8000 Å was a factor of about 1.5. Above

8000 Å, the factor rises to a peak of 7 at 9500 Å. Thicker silicon gives the new CCD comparatively excellent sensitivity to far-red light. The throughput of the upgraded spectrograph peaks at 37% with the 158/7560 grating. The peak is not as large for the 600/9500 grating due to its redder blaze wavelength.

Figure 5 also demonstrates the increase in spectral range afforded by the new detector. The new CCD has four times as many pixels as the previous detector, but the new pixels are 5/8 as large. Therefore, the spectral range is 2.5 times larger. With the 600/9500 grating, the spectral range increased from 1340 Å to 3350 Å. However, the optical quality varies over the CCD. The red camera was not designed for such a large detector. As a result, the image quality suffers near the ends of the chip, especially the red end. Figure 3 shows that the apparent widths of arc lines increase with wavelength. The extra width is caused not by de-focusing, but by multiple images of the arc lines.

The new red channel meets all of the requirements in Section 3 except the mandate for a read noise of $< 3 e^-$. We installed electromagnetic shielding to reduce the noise, but it remains at $8 e^-$, and there is some structure to the noise in a bias frame. We identified some possible courses of action, but we, in consultation with the administration of Caltech Optical Observatories, decided to release the instrument for science.

6. Summary

The detector in the red channel of the Palomar Double Spectrograph was last replaced in 1995. In order to modernize the instrument and extend its capabilities, we replaced the old detector with an LBNL deep-depletion CCD. This upgrade improved the throughput of the spectrograph by a factor of 1.5 below

8000 Å. The thick CCD is also exceptionally sensitive to far-red light. The useful spectral range of DBSP now extends to well beyond 1 μm . The new chip is 2.5 longer than the previous chip, allowing for a wider spectral range in a single exposure, although the reddest quarter of the spectrum suffers from optical aberrations.

The new detector entered service for science observations the same day that it was commissioned. All presently scheduled and future DBSP observers may enjoy the new capabilities offered by this spectrograph.

This upgrade would not have been possible without the hard work of the talented staff of Palomar Observatory and Caltech Optical Observatories, including Andy Boden, Khanh Bui, Ernest Croner, Rich Dekany, Mike Doyle, Carolyn Heffner, Jeff Hickey, Steve Kunsman, Dan McKenna, Jennifer Milburn, Jean Mueller, Kajsa Peffer, Kevin Rykoski, Roger Smith, Viswa Velur, and Jeff Zolkower. We also thank Judy Cohen for her advice throughout the upgrade and for her input to this manuscript.

Support for this work was provided by NASA through Hubble Fellowship grant 51256.01 awarded to ENK by the Space Telescope Science Institute, which is operated by the Association of Universities for Research in Astronomy, Inc., for NASA, under contract NAS 5-26555.

REFERENCES

- Bhalerao, V. B., van Kerkwijk, M. H., Harrison, F. A., et al. 2010, *ApJ*, 721, 412
- Buratti, B. J., Hicks, M. D., Tryka, K. A., Sittig, M. S., & Newburn, R. L. 2002, *Icarus*, 155, 375
- Burgasser, A. J., Kirkpatrick, J. D., Liebert, J., & Burrows, A. 2003, *ApJ*, 594, 510
- Hayes, D. S., & Latham, D. W. 1975, *ApJ*, 197, 593
- Hillenbrand, L. A., Foster, J. B., Persson, S. E., & Matthews, K. 2002, *PASP*, 114, 708
- Kirkpatrick, J. D., Reid, I. N., Liebert, J., et al. 1999, *ApJ*, 519, 802
- Massey, P., & Gronwall, C. 1990, *ApJ*, 358, 344
- Massey, P., Strobel, K., Barnes, J. V., & Anderson, E. 1988, *ApJ*, 328, 315
- Nordh, H. L., Lindgren, B., & Wing, R. F. 1977, *A&A*, 56, 1
- Oke, J. B. 1990, *AJ*, 99, 1621
- Oke, J. B., Cohen, J. G., Carr, M., et al. 1995, *PASP*, 107, 375
- Oke, J. B., & Gunn, J. E. 1982, *PASP*, 94, 586
- Rockosi, C., Stover, R., Kibrick, R., et al. 2010, *Proc. SPIE*, 7735
- Thatte, N., Tecza, M., Clarke, F., et al. 2010, *Proc. SPIE*, 7735
- van Dokkum, P. G., & Conroy, C. 2010, *Nature*, 468, 940
- Weaver, J. H., & Frederikse, H. P. R. 2010, "Optical Properties of Selected Elements," in *CRC Handbook of Chemistry and Physics*, 92nd Edition (Internet Version 2010), W. M. Haynes, ed., CRC Press/Taylor and Francis, Boca Raton, FL
- Weissman, P. R., Hicks, M. D., Abell, P. A., Choi, Y.-J., & Lowry, S. C. 2008, *Meteoritics and Planetary Science*, 43, 905
- Whitford, A. E. 1977, *ApJ*, 211, 527

Wing, R. F., Cohen, J., & Brault, J. W. 1977,
ApJ, 216, 659

Wing, R. F., & Ford, W. K., Jr. 1969, PASP,
81, 527

Wu, Y., Shi, Y., Helou, G., et al. 2011, ApJ,
734, 40